

Impact of H_0 prior on the evidence for dark radiationErminia Calabrese,¹ Maria Archidiacono,² Alessandro Melchiorri,² and Bharat Ratra³¹*Sub-department of Astrophysics, Denys Wilkinson Building, University of Oxford, Keble Road, Oxford OX1 3RH, United Kingdom*²*Physics Department and INFN, Università di Roma “La Sapienza”, Ple Aldo Moro 2, 00185 Rome, Italy*³*Department of Physics, Kansas State University, 116 Cardwell Hall, Manhattan KS 66506, USA*

(Received 7 June 2012; published 15 August 2012)

Recent analyses that include cosmic microwave background (CMB) anisotropy measurements from the Atacama Cosmology Telescope and the South Pole Telescope have hinted at the presence of a dark radiation component at more than two standard deviations. However, this result depends sensitively on the assumption of an Hubble Space Telescope prior on the Hubble constant, where $H_0 = 73.8 \pm 2.4$ km/s/Mpc at 68% c.l.. Here we repeat this kind of analysis assuming a prior of $H_0 = 68 \pm 2.8$ km/s/Mpc at 68% c.l., derived from a median statistics (MS) analysis of 537 non-CMB H_0 measurements from Huchra’s compilation. This prior is fully consistent with the value of $H_0 = 69.7 \pm 2.5$ km/s/Mpc at 68% c.l. obtained from CMB measurements under assumption of the standard Λ CDM model. We show that with the MS H_0 prior the evidence for dark radiation is weakened to ~ 1.2 standard deviations. Parametrizing the dark radiation component through the effective number of relativistic degrees of freedom N_{eff} , we find $N_{\text{eff}} = 3.98 \pm 0.37$ at 68% c.l. with the Hubble Space Telescope prior and $N_{\text{eff}} = 3.52 \pm 0.39$ at 68% c.l. with the MS prior. We also discuss the implications for current limits on neutrino masses and on primordial Helium abundances.

DOI: [10.1103/PhysRevD.86.043520](https://doi.org/10.1103/PhysRevD.86.043520)

PACS numbers: 98.70.Vc

I. INTRODUCTION

Recent measurements of the cosmic microwave background (CMB) radiation anisotropy made by the Atacama Cosmology Telescope (ACT) [1] and by the South Pole Telescope (SPT) [2] have provided valuable general confirmation of the theoretical predictions of the shape of the CMB anisotropy at arcminute angular scales, in the diffusion damping regime.

While the inclusion of these new small-scale data do not significantly alter the constraints on parameters of the “standard” Λ CDM cosmological model [3,4], compared to those obtained by using the Wilkinson Microwave Anisotropy Probe (WMAP) satellite CMB anisotropy data in conjunction with other cosmological measurements [5], they can be used to significantly improve the constraints on those new, “beyond-standard-model,” parameters that mostly affect the physics of the CMB anisotropy diffusion damping tail.

In particular, the recent ACT and SPT data have placed new constraints on the number of relativistic degrees of freedom, N_{eff} , that define the physical energy density in relativistic particles today, ρ_{rad} , given by

$$\rho_{\text{rad}} = \left[1 + \frac{7}{8} \left(\frac{4}{11} \right)^{4/3} N_{\text{eff}} \right] \rho_{\gamma}, \quad (1)$$

where ρ_{γ} is the energy density of the CMB photons at present temperature $T_{\gamma} = 2.726$ K (see, e.g., Ref. [6]). In the standard scenario, assuming three active massless neutrino species with standard electroweak interactions, the expected value is $N_{\text{eff}} = 3.046$, slightly larger than 3

because of non-instantaneous neutrino decoupling (see, e.g., Ref. [7]).

The new data from ACT and SPT, jointly analyzed with earlier, large-scale WMAP (and other) data, rule out the case of $N_{\text{eff}} = 0$ at high statistical significance. That is, for the first time, CMB anisotropy and large-scale structure observations confirm the existence of neutrinos.¹ However, these data also seem to prefer a value of $N_{\text{eff}} \sim 4$, hinting at the presence of an additional relativistic component (see Refs. [1,2]), over and above the three neutrino species in the standard model of particle physics. In particular, some of us, [8], found $N_{\text{eff}} = 4.08^{+0.71}_{-0.68}$ at 95% confidence level from such an analysis and similar results are presented in Refs. [9,10].

These results are significant, since they rather strongly suggest that CMB anisotropy data (alone or in conjunction with other large-scale cosmological data) indicate the presence of some kind of “dark radiation” that is not seen in any other cosmological data. They have prompted the development of many theoretical models in which N_{eff} is larger than 3, [11].

Several nonstandard models related to axions or decaying particles, gravity waves, extra dimensions, and dark energy [12] can in fact predict a larger value for N_{eff} .

It is therefore crucial to carefully investigate this result, to see if it can be strengthened or weakened by, for example, considering a slightly different choice of data.

¹Of course, cosmological big bang nucleosynthesis theory in combination with the observed light nuclei abundances had pointed to this earlier.

It is well known in the literature (see, e.g., Refs. [8,9]) that N_{eff} is degenerate with the value of the Hubble constant H_0 . Assuming a prior on the value of the Hubble constant is therefore a key step in the determination of N_{eff} from the data. The prior on the Hubble constant used in most recent analyses, labeled HST, is a Gaussian one based on the results of Ref. [13] with $H_0 = 73.8 \pm 2.4$ km/s/Mpc, including systematics.

While this 3% determination of H_0 is certainly impressive, one might wonder if a slightly different Hubble constant prior could change the preference for $N_{\text{eff}} > 3$. There are several indications that a different Hubble constant prior could be more appropriate. For instance, a number of measurements result in a significantly lower value of H_0 ; e.g., the Ref. [14] summary value is $H_0 = 62.3 \pm 4$ km/s/Mpc. In addition, a standard analysis, under the assumption of $N_{\text{eff}} = 3.046$, of CMB data alone is able (in a flat universe) to constrain the Hubble constant. Recent such analyses yield $H_0 \sim 70$ km/s/Mpc, more than one standard deviation away from the HST value. For example, the analysis of ACT and WMAP7 data in Ref. [1] gives $H_0 = 69.7 \pm 2.5$ km/s/Mpc. Clearly, there is also observational evidence for a significantly smaller value of H_0 than the HST estimate. Furthermore, it is possible that using a prior with a lower value of H_0 could result in a N_{eff} determined from CMB anisotropy and other large-scale data that is consistent with the other cosmological N_{eff} determinations.

There are very many measurements of H_0 , over 550.² Most recent estimates lie in the interval 60–75 km/s/Mpc, with error bars on some individual estimates probably being too small, since these measurements are mutually inconsistent (this is likely a consequence of underestimated systematic errors in some cases). Clearly, what is needed is a convincing summary observational estimate of H_0 .³ To date, the best technique for deriving such a summary estimate—that does not make use of the error bars of the individual measurements—is the median statistics technique; Ref. [16] includes a detailed description of this technique.

The median statistics technique has been used to analyze a number of cosmological data sets. These include Type Ia supernova apparent magnitude data, to show that the current cosmological expansion is accelerating, [16,17]; CMB temperature anisotropy data, in one of the first analyses to show that these data were consistent with flat spatial hypersurfaces, [18]; and, collections of measurements of the cosmological clustered mass density, in one of the earliest analyses to show that this makes up around 25–30% of the current epoch cosmological energy budget, [19]. These successes support the idea that a median statistics estimate of the Hubble constant provides an accurate summary estimate.

The median statistics technique has been used thrice to analyse Huchra’s list (at three different epochs). From an analysis of 331 measurements (up to the middle of 1999), Ref. [16] found a median statistics summary $H_0 = 67$ km/s/Mpc; from 461 measurements (up to the middle of 2003), and from 553 measurements (up to early 2011), Refs. [20,21] both found a median statistics summary $H_0 = 68$ km/s/Mpc. While the estimated statistical error bar (given by the scatter in the central H_0 values) has decreased as the sample size has increased, the larger (and dominant) systematic error bar (estimated from the scatter in the summary values of H_0 determined by different techniques) has changed much less.

For our analyses here we estimate H_0 using the method of Ref. [21] but now excluding from the Huchra list of 553 measurements the 16 H_0 measurements derived from CMB data assuming $N_{\text{eff}} = 3.046$. We exclude these 16 CMB measurements as we want an external and independent prior on H_0 to use in our analysis of the latest CMB datasets. From a median statistics analysis of the 537 non-CMB measurements we find $H_0 = 68 \pm 2.8$ km/s/Mpc (one standard deviation error), identical to that found in Ref. [21] from an analysis of the 553 measurements. In what follows we refer to the Gaussian prior based on this value as the median statistics (MS) H_0 prior.

Our goal here is to discuss the implications of assuming the MS prior for H_0 , instead of the usual HST prior, for current CMB and large-scale structure parameter inference. We focus much of our attention on the value of N_{eff} and the evidence for dark radiation, but we also consider how the MS prior changes the estimated value of other parameters, including the dark energy equation of state parameter w and the spectral index of primordial fluctuations n_s .

Our paper is organized as follows. In the next section we briefly summarize the data analysis method we use. In Sec. III we present our results. We conclude in Sec. IV.

II. ANALYSIS METHOD

Our analysis is based on a modified version of the public COSMOMC [22] Monte Carlo Markov Chain code. We include the following CMB data: WMAP7 [5], ACBAR [23], ACT [1], and SPT [2], including measurements up to maximum multipole number $l_{\text{max}} = 3000$. As in Ref. [8] we include galaxy clustering data from the SDSS-DR7 luminous red galaxy sample [24]. Also, as discussed in the Introduction, we choose two different priors on the Hubble constant: the median statistics (MS) prior of $H_0 = 68 \pm 2.8$ km/s/Mpc as well as, for comparison, the HST prior [13] used in previous analyses.

In the basic analysis we sample the usual seven-dimensional set of cosmological parameters, adopting flat priors on them: the baryon and cold dark matter densities $\Omega_b h^2$ and $\Omega_c h^2$, the ratio of the sound horizon to the angular diameter distance at decoupling θ , the optical

²See cfa-www.harvard.edu/~huchra/.

³And not just for the case at hand, but for many different cosmological parameter analyses, see, e.g., Refs. [15].

depth to reionization τ , the scalar spectral index n_s , the overall normalization of the spectrum A_s at $k = 0.002 \text{ Mpc}^{-1}$, the effective number of relativistic degrees of freedom N_{eff} .

Our analysis is very similar to the one presented in Ref. [8], with three changes: (i) we consider two different H_0 priors; (ii) we consider an extended case where we assume massive neutrinos, we enlarge our parameter space varying the total mass of neutrinos $\sum m_\nu$; (iii) we allow the Helium abundance Y_p to vary consistently with standard BBN following Ref. [2]. This means that each theoretical CMB angular spectrum is computed assuming a value for Y_p derived by BBN nucleosynthesis from the input values of $\Omega_b h^2$ and N_{eff} of the theoretical model considered. The small uncertainty on Y_p derived from the experimental errors on the neutron half-life produces negligible changes in the CMB angular spectra so we ignore it. In a latter case we also vary Y_p as a free parameter.

In addition, where indicated, we also present constraints on the dark energy equation of state parameter w (the ratio of the pressure to energy density of the dark energy fluid), assumed to be redshift independent, although the corresponding dark energy density is time dependent.⁴ We consider massless neutrinos, adiabatic initial conditions, and a spatially-flat universe.

Following Ref. [8] we account for foreground contributions by marginalizing over three additional amplitudes: the Sunyaev-Zeldovich effect amplitude A_{SZ} , the amplitude of clustered point sources A_C , and the amplitude of Poisson-distributed point sources A_P .

III. RESULTS

A. Neutrinos

As in Ref. [8], we compute the likelihood function in the seven-dimensional (or eight when massive neutrinos are considered) cosmological parameter space described above, and multiply it by the prior probability distribution functions to derive the seven-dimensional posterior probability density distribution function. Marginalizing this over all but one of the cosmological parameters gives the one-dimensional posterior probability distribution function for the parameter of interest. This one-dimensional

⁴This is the widely-used Λ CDM parametrization of dark energy. It is not a complete parametrization, as it cannot describe the evolution of spatial inhomogeneities, nor is it an accurate approximation of more physically motivated time-varying dark energy models, [25]. It is preferable to use a consistent and physically motivated dark energy model, e.g., that proposed in Refs. [26], for such an analysis, but this is a much more involved undertaking, so instead we patch up the Λ CDM parametrization by assuming that the acoustic spatial inhomogeneities travel at the speed of light. This extended Λ CDM parametrization should provide reasonable (qualitative) indications of what might be expected in a consistent, physically motivated model of time-varying dark energy.

distribution function is used to determine the most likely value of the parameter, as well as limits on it. These are listed in Table I, for three different Hubble constant priors: a flat one (no prior); the Gaussian HST one, [13]; and the Gaussian MS one. Marginalizing over only five of the cosmological parameters, we derive the two-dimensional posterior probability density distribution function $P(H_0, N_{\text{eff}})$. This is used to derive the constraint contours in the two-dimensional $N_{\text{eff}}-H_0$ parameter space shown in Fig. 1, for the two Gaussian H_0 priors.

Table I and Fig. 1 show that the H_0 prior plays a crucial role in determining constraints on N_{eff} from the data. With the HST H_0 prior we find a central N_{eff} value that is 2.5σ larger than 3.046, while the median statistics prior results in an N_{eff} that is consistent with 3.046 (being only 1.2σ larger).

The HST prior is therefore at least partially responsible for the current indication for dark radiation. However, as we can see from the central values of H_0 and N_{eff} obtained when a flat prior on H_0 is assumed, the CMB anisotropy and large-scale structure data considered here prefers a larger value of N_{eff} (being 1.9σ larger than 3.046) and a somewhat larger value of H_0 . This is clear also from the χ^2_{min} values of the best fit that are higher when the median statistics H_0 prior is assumed, compared to the case of the HST prior (see the last line of Table I).

The H_0 prior is crucial also in the determination of the $\sum m_\nu$ limits if we instead limit ourselves to the case of 3, standard, massive neutrinos. In Table I, columns 3 and 5, we quote the cosmological parameters and the upper limits on $\sum m_\nu$ in case of the HST and of the MS prior. As we can see, the upper limit on $\sum m_\nu$ is considerably weaker when the MS prior is considered, with the 95% c.l. upper limit moving from $\sum m_\nu < 0.36 \text{ eV}$ in the case of the HST prior to $\sum m_\nu < 0.60 \text{ eV}$ in the case of the MS prior. This can be clearly explained by the CMB degeneracy between H_0 and $\sum m_\nu$ as illustrate in Fig. 2. Namely, lower values of the Hubble parameter are in better agreement with current CMB data when $\sum m_\nu$ is increased. Data set preferring higher values for H_0 will therefore provide stronger constraints on $\sum m_\nu$ when combined with the CMB data.

Beside the $N_{\text{eff}}-H_0$ degeneracy, it is interesting to note that there also is a degeneracy between N_{eff} and n_s . When the HST prior is assumed, n_s is 1.8σ below 1, while for the median statistics case it is 3σ below unity.

In Fig. 3 we show the contours in the two-dimensional $\Omega_m-\sigma_8$ parameter space, for the two Gaussian H_0 priors. Here σ_8 is the amplitude of density inhomogeneities averaged over spheres of radius $8h^{-1} \text{ Mpc}$. In this figure we also show the fit to the central value and the two standard deviation limits of the constraint from the normalization of the galaxy cluster mass function from Ref. [27], i.e., $\sigma_8 = (0.25/\Omega_m)^{0.47}[0.813 \pm 0.013 \pm 0.024]$. Here the first error bar represents the statistical, and the second the systematic, error (see their Sec. 10). We derive the 2σ

TABLE I. Cosmological parameter values and 68% confidence level errors assuming N_{eff} relativistic neutrinos or $N_{\text{eff}} = 3.046$ massive neutrinos. 95% c.l. upper bounds are listed for the sum of neutrino masses and foregrounds parameters. We also list the derived Hubble constant, the nonrelativistic matter density parameter $\Omega_m = \Omega_c + \Omega_b$, and σ_8 , the amplitude of density inhomogeneities averaged over spheres of radius $8h^{-1}$ Mpc, where h is the Hubble constant in units of 100 km/s/Mpc.

| Parameters | No Prior | HST Prior | | MS Prior | |
|--------------------------|-----------------------|-------------------------|-----------------------|-----------------------|-----------------------|
| | | 73.8 ± 2.4 km/s/Mpc | | 68 ± 2.8 km/s/Mpc | |
| $\Omega_b h^2$ | 0.02258 ± 0.00050 | 0.02248 ± 0.00039 | 0.02210 ± 0.00037 | 0.02211 ± 0.00040 | 0.02188 ± 0.00036 |
| $\Omega_c h^2$ | 0.134 ± 0.010 | 0.1317 ± 0.0080 | 0.1142 ± 0.0029 | 0.1256 ± 0.0080 | 0.1181 ± 0.0032 |
| θ | 1.0395 ± 0.0016 | 1.0397 ± 0.0016 | 1.0415 ± 0.0014 | 1.0400 ± 0.0017 | 1.0409 ± 0.0014 |
| τ | 0.085 ± 0.014 | 0.084 ± 0.013 | 0.083 ± 0.013 | 0.080 ± 0.013 | 0.081 ± 0.014 |
| n_s | 0.984 ± 0.017 | 0.979 ± 0.012 | 0.9659 ± 0.0091 | 0.964 ± 0.012 | 0.9536 ± 0.0090 |
| N_{eff} | 4.14 ± 0.57 | 3.98 ± 0.37 | 3.046 | 3.52 ± 0.39 | 3.046 |
| $\sum m_\nu [\text{eV}]$ | 0.0 | 0.0 | <0.36 | 0.0 | <0.60 |
| $H_0 [\text{km/s/Mpc}]$ | 75.2 ± 3.6 | 74.2 ± 2.0 | 69.3 ± 1.4 | 70.9 ± 2.1 | 66.8 ± 1.8 |
| $\log(10^{10} A_s)$ | 3.183 ± 0.043 | 3.191 ± 0.035 | 3.205 ± 0.034 | 3.219 ± 0.036 | 3.226 ± 0.034 |
| Ω_m | 0.277 ± 0.019 | 0.280 ± 0.016 | 0.284 ± 0.017 | 0.294 ± 0.017 | 0.315 ± 0.024 |
| σ_8 | 0.882 ± 0.033 | 0.876 ± 0.028 | 0.782 ± 0.032 | 0.857 ± 0.028 | 0.757 ± 0.043 |
| A_{SZ} | <1.4 | <1.3 | <0.97 | <1.1 | <0.96 |
| $A_c [\mu\text{K}^2]$ | <14.5 | <14.7 | <12.8 | <14.1 | <13.1 |
| $A_p [\mu\text{K}^2]$ | <24.9 | <25.5 | <26.6 | <26.1 | <26.6 |
| χ^2_{min} | 7593.4 | 7593.2 | 7592.0 | 7594.8 | 7595.1 |

cluster constraints shown in Fig. 2 by adding these errors in quadrature and then doubling.

From Fig. 3 we see that both H_0 priors give results that are not far off from what the measured normalization of the cluster mass function demands. Qualitatively, the HST H_0 prior is more consistent with the cluster data if $\Omega_m \sim 0.25$, near the low end of current indications, see, e.g., Ref. [19], while the median statistics case prefers a larger $\Omega_m \sim 0.27$, more consistent with current measurements, see, e.g., Ref. [19].

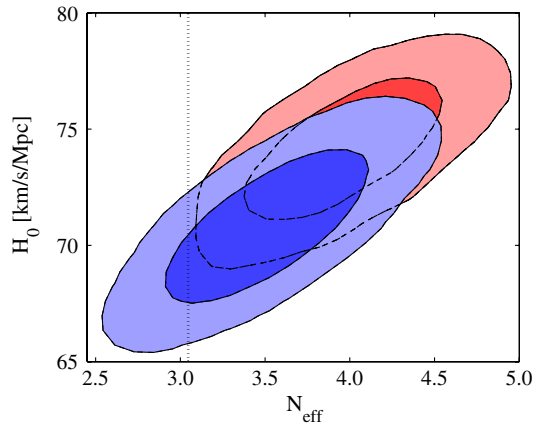


FIG. 1 (color online). Constraints in the $N_{\text{eff}}-H_0$ plane. Elliptical two-dimensional posterior probability distribution function contours show the 68% and 95% c.l. limits. Red contours and regions (closer to the upper right corner) assume the HST prior with $H_0 = 73.4 \pm 2.4$ km/s/Mpc, while blue contours and regions (closer to the lower left corner) are obtained using the median statistics prior with $H_0 = 68 \pm 2.8$ km/s/Mpc. The dotted black vertical line corresponds to $N_{\text{eff}} = 3.046$.

B. Helium mass abundance

One assumption made in the previous paragraph is that the Helium abundance is varied consistently with BBN. Current CMB data produce only weak constraints on this quantity and allowing Y_p to vary freely would make the standard case of $N_{\text{eff}} = 3.046$ in better agreement with data due to an anticorrelation between N_{eff} and Y_p in CMB data (see, for example, the discussion in [28]). In order to check the impact of the H_0 priors in this case, we have performed

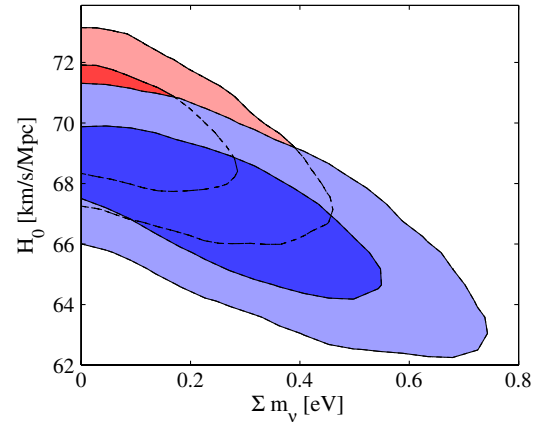


FIG. 2 (color online). Constraints in the $\sum m_\nu-H_0$ plane. Elliptical two-dimensional posterior probability distribution function contours show the 68% and 95% c.l. limits. Red contours and regions (closer to the upper left corner) assume the HST prior with $H_0 = 73.4 \pm 2.4$ km/s/Mpc, while blue contours and regions (closer to the lower right corner) are obtained using the median statistics prior with $H_0 = 68 \pm 2.8$ km/s/Mpc.

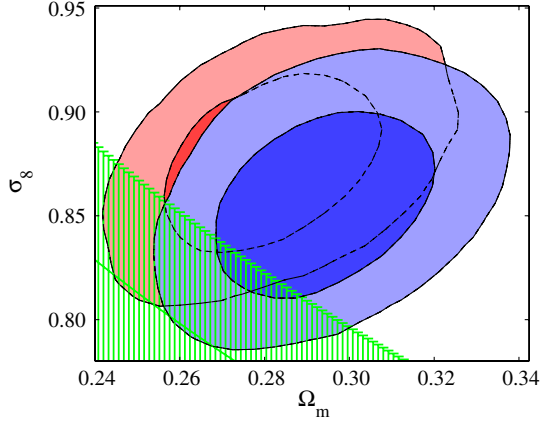


FIG. 3 (color online). Constraints in the Ω_m - σ_8 plane. Elliptical two-dimensional posterior probability density function contours show the 68% and 95% confidence level limits. Red contours (closer to the upper left corner) assume the HST prior with $H_0 = 73.8 \pm 2.4$ km/s/Mpc; blue contours (closer to the lower right corner) are obtained with the median statistics prior where $H_0 = 68 \pm 2.8$ km/s/Mpc. The green region (in the lower left corner) demarcates the central value and 2σ limits from the cluster mass function normalization data, [27].

two analysis varying the Helium abundance Y_p and N_{eff} . The results are reported in Table II.

As we can see, when Y_p is allowed to vary, the standard case of N_{eff} is more consistent with current data in both cases. In the case of the MS prior we have $N_{\text{eff}} = 2.75 \pm 0.46$ that is perfectly consistent with the expectations of the standard scenario. However, the value obtained for the Helium abundance is probably too high in the case of the MS prior: $Y_p = 0.334 \pm 0.033$, that is about two standard deviations away from the conservative experimental bound

TABLE II. Cosmological parameter values derived assuming a varying Y_p . Errors are at 68% c.l. while upper bounds at 95% c.l. are reported for foregrounds parameters.

| Parameters | HST Prior | MS Prior |
|-----------------------|-----------------------|-----------------------|
| $\Omega_b h^2$ | 0.02274 ± 0.00042 | 0.02246 ± 0.00043 |
| $\Omega_c h^2$ | 0.1246 ± 0.0091 | 0.1138 ± 0.0085 |
| θ | 1.0429 ± 0.0027 | 1.0454 ± 0.0029 |
| τ | 0.087 ± 0.014 | 0.085 ± 0.014 |
| n_s | 0.986 ± 0.013 | 0.972 ± 0.013 |
| N_{eff} | 3.52 ± 0.48 | 2.75 ± 0.46 |
| H_0 [km/s/Mpc] | 72.7 ± 2.2 | 68.2 ± 2.3 |
| Y_p | 0.310 ± 0.034 | 0.334 ± 0.033 |
| $\log(10^{10} A_s)$ | 3.175 ± 0.037 | 3.197 ± 0.036 |
| Ω_m | 0.279 ± 0.015 | 0.293 ± 0.016 |
| σ_8 | 0.872 ± 0.029 | 0.847 ± 0.029 |
| A_{SZ} | <1.7 | <1.6 |
| $A_c [\mu\text{K}^2]$ | <15.4 | <15.3 |
| $A_p [\mu\text{K}^2]$ | <23.1 | <23.4 |
| χ^2_{min} | 7592.0 | 7590.4 |

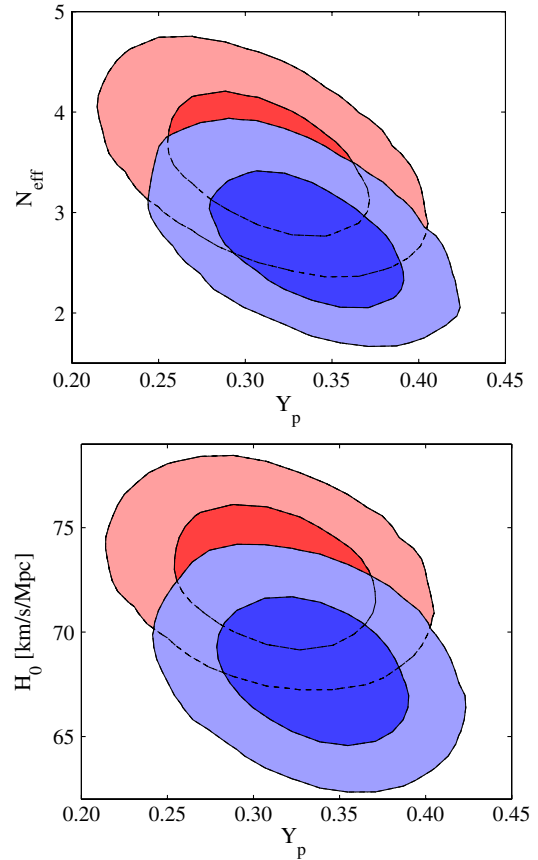


FIG. 4 (color online). Constraints in the Y_p - N_{eff} plane (top) and Y_p - H_0 (bottom). Elliptical two-dimensional posterior probability distribution function contours show the 68% and 95% c.l. limits. Red contours and regions (closer to the upper left corner) assume the HST prior with $H_0 = 73.4 \pm 2.4$ km/s/Mpc, while blue contours and regions (closer to the lower right corner) are obtained using the median statistics prior with $H_0 = 68 \pm 2.8$ km/s/Mpc.

of $Y_p < 0.2631$ obtained from an analysis of direct measurements in [29].

The larger helium abundance obtained in the case of the MS prior respect to the HST prior can be clearly seen from the direction of the degeneracies in the 2D contours plots in Figure 4. Namely, a lower N_{eff} prefers a higher Y_p and a lower prior for H_0 shifts the constraints toward lower N_{eff} and higher values for Y_p .

C. Λ CDM

The standard Λ CDM cosmological model has some conceptual problems that are partially alleviated in some models in which the dark energy density varies slowly in time (and so weakly in space), [26]. Furthermore, observational constraints on cosmological parameters are model dependent, i.e., the observational estimate of a cosmological parameter, e.g., N_{eff} , depends on the cosmological model used to analyze the data. It is therefore of interest to examine the observational cosmological constraints on

TABLE III. Cosmological parameter values derived assuming the XCDM parametrization of time-evolving dark energy. Errors are at 68% c.l. while upper bounds at 95% c.l. are reported for foregrounds parameters.

| Parameters | HST Prior | | MS Prior | |
|-----------------------|-----------------------|----------------------|-----------------------|-----------------------|
| $\Omega_b h^2$ | 0.02200 ± 0.00040 | 0.02290 ± 0.0054 | 0.02206 ± 0.00040 | 0.02279 ± 0.00053 |
| $\Omega_c h^2$ | 0.1162 ± 0.0039 | 0.1347 ± 0.0085 | 0.1141 ± 0.0040 | 0.1291 ± 0.0084 |
| θ | 1.0414 ± 0.0015 | 1.0396 ± 0.0016 | 1.0414 ± 0.0015 | 1.0400 ± 0.0016 |
| τ | 0.080 ± 0.013 | 0.089 ± 0.015 | 0.081 ± 0.013 | 0.089 ± 0.015 |
| n_s | 0.956 ± 0.010 | 0.997 ± 0.019 | 0.959 ± 0.011 | 0.993 ± 0.019 |
| N_{eff} | 3.046 | 4.42 ± 0.54 | 3.046 | 4.16 ± 0.53 |
| H_0 [km/s/Mpc] | 72.1 ± 2.4 | 72.8 ± 2.3 | 66.7 ± 2.6 | 68.0 ± 2.4 |
| w | -1.09 ± 0.10 | -0.86 ± 0.11 | -0.90 ± 0.10 | -0.76 ± 0.10 |
| $\log(10^{10} A_s)$ | 3.223 ± 0.039 | 3.150 ± 0.050 | 3.210 ± 0.041 | 3.149 ± 0.051 |
| Ω_m | 0.267 ± 0.018 | 0.298 ± 0.022 | 0.307 ± 0.226 | 0.329 ± 0.025 |
| σ_8 | 0.856 ± 0.044 | 0.831 ± 0.047 | 0.790 ± 0.046 | 0.775 ± 0.047 |
| A_{SZ} | <0.94 | <1.5 | <0.95 | <1.4 |
| $A_c[\mu\text{K}^2]$ | <13.0 | <15.0 | <13.0 | <14.9 |
| $A_p[\mu\text{K}^2]$ | <27.0 | <23.9 | <26.7 | <24.7 |
| χ^2_{min} | 7598.1 | 7592.7 | 7595.1 | 7592.1 |

N_{eff} in a cosmological model in which the dark energy density varies in time, such as that of Ref. [26]. This is a somewhat challenging task that we will leave for future work. However, to get an indication of what could be expected from such an analysis, we determine the observational constraints on N_{eff} in a cosmological model in which the time-evolving dark energy density is parametrized by the XCDM parametrization (made complete by assuming that the acoustic spatial inhomogeneities propagate at the speed of light) described above. Table III shows the observational constraints derived under these assumptions.

From Table III we see that the MS prior changes the best fit w in the standard case with $N_{\text{eff}} = 3.046$ to $w \sim -0.9$, with $w = -1$ off by one standard deviation. When both w and N_{eff} are allowed to vary freely, the geometrical

degeneracy with H_0 makes the HST and MS H_0 priors much less effective. In this case the evidence for dark radiation is again significant: for the MS H_0 prior case we find $N_{\text{eff}} = 4.16 \pm 0.53$, and a dark energy equation of state parameter $w = -0.76 \pm 0.10$, i.e., excluding a cosmological constant at more than two standard deviations. A scale-invariant HPYZ primordial spectrum with $n_s = 1$ is fully consistent with both priors. While some of these values indicate significant tensions with the standard Λ CDM model, it is important to keep in mind the strong degeneracies between N_{eff} , H_0 , and w , as well as the fact that the XCDM parametrization used in the analysis has been arbitrarily completed to allow for an accounting of the evolution of density inhomogeneities.

In order to try to break these degeneracies, and derive more reliable constraints on the parameters, we perform a

TABLE IV. Similar constraints as in Table III, but now also including the SNeIa data in the analysis.

| Parameters | HST Prior + SNeIa | | MS Prior + SNeIa | |
|-----------------------|-----------------------|-----------------------|-----------------------|-----------------------|
| $\Omega_b h^2$ | 0.02203 ± 0.00038 | 0.02260 ± 0.00046 | 0.02190 ± 0.00038 | 0.02230 ± 0.00046 |
| $\Omega_c h^2$ | 0.1156 ± 0.0037 | 0.1317 ± 0.0079 | 0.1157 ± 0.0038 | 0.1249 ± 0.0077 |
| θ | 1.0414 ± 0.0015 | 1.0400 ± 0.0016 | 1.0411 ± 0.0015 | 1.0401 ± 0.0016 |
| τ | 0.081 ± 0.013 | 0.086 ± 0.014 | 0.080 ± 0.013 | 0.083 ± 0.014 |
| n_s | 0.957 ± 0.010 | 0.985 ± 0.015 | 0.956 ± 0.010 | 0.972 ± 0.016 |
| N_{eff} | 3.046 | 4.08 ± 0.43 | 3.046 | 3.63 ± 0.42 |
| H_0 [km/s/Mpc] | 71.0 ± 1.6 | 74.0 ± 2.0 | 68.8 ± 1.6 | 70.6 ± 2.1 |
| w | -1.050 ± 0.069 | -0.967 ± 0.075 | -0.989 ± 0.070 | -0.946 ± 0.076 |
| $\log(10^{10} A_s)$ | 3.222 ± 0.038 | 3.178 ± 0.043 | 3.221 ± 0.038 | 3.198 ± 0.044 |
| Ω_m | 0.273 ± 0.014 | 0.282 ± 0.015 | 0.291 ± 0.015 | 0.295 ± 0.016 |
| σ_8 | 0.843 ± 0.035 | 0.863 ± 0.038 | 0.823 ± 0.036 | 0.836 ± 0.038 |
| A_{SZ} | <0.94 | <1.3 | <0.94 | <1.2 |
| $A_c[\mu\text{K}^2]$ | 13.0 | 14.8 | <13.1 | <14.0 |
| $A_p[\mu\text{K}^2]$ | 27.0 | 24.8 | <27.0 | <26.0 |
| χ^2_{min} | 8128.4 | 8124.0 | 8126.2 | 8125.6 |

new analysis that also include the SDSS supernova Type Ia (SNeIa) apparent magnitude data, [30]. From Table IV we see that the inclusion of the SNeIa data bring the results back to the previous dichotomy: the HST prior clearly shows a preference for $N_{\text{eff}} > 3.046$ while the MS prior results in a value of N_{eff} that is in much better agreement with the standard scenario. The constraints on the equation of state are $w = -0.967 \pm 0.075$ for the HST prior and $w = -0.946 \pm 0.076$ for the MS prior. The HPYZ spectrum with $n_s = 1$ is again in tension with the observations for the MS H_0 prior at a little less than two standard deviations.

IV. CONCLUSIONS

A “standard” cosmological model is starting to fall in place. Interestingly, recent data have provided some indication for an unexpected new “dark radiation” component. In this brief paper we have again emphasized the important role played by the HST H_0 prior in establishing the statistical evidence for the existence of this dark radiation. We have also shown that with a new median statistics H_0 prior derived from 537 non-CMB H_0 measurements, there is no significant evidence for $N_{\text{eff}} > 3.046$, consistent with the indications from other cosmological data. And it is probably not unreasonable to believe that the converse might also be true: with other cosmological data not inconsistent with $N_{\text{eff}} = 3.046$,

consistency of the smaller-scale CMB anisotropy data with the predictions of the Λ CDM model apparently demands $H_0 \sim 68$ km/s/Mpc.

We emphasize, however, that when the same data are analysed in the context of the somewhat arbitrarily-completed XCDM dark energy parametrization, they prefer $N_{\text{eff}} > 3.046$. It would be useful to see if this remains the case if, instead of XCDM, a complete and consistent model, such as ϕ CDM, is used in the analysis.

We have shown that the HST H_0 prior is, at least partially, responsible for the evidence supporting the existence of a new dark radiation component. However, future CMB anisotropy and galaxy clustering data, as well as a definitive determination of H_0 , will be needed to fully resolve this issue.

In particular, the future data expected from the Planck satellite should be able to constrain independently the values of H_0 and N_{eff} , clarifying if the current tension between the HST and CMB constraints on H_0 is due to a dark radiation component or systematics in the data.

ACKNOWLEDGMENTS

This work is supported by PRIN-INAF “Astronomy probes fundamental physics”, the Italian Space Agency through ASI Contract Euclid-IC (I/031/10/0), DOE Grant No. DEFG030-99EP41093, and NSF Grant No. AST-1109275.

-
- [1] J. Dunkley *et al.*, *Astrophys. J.* **739**, 52 (2011).
 [2] R. Keisler *et al.*, *Astrophys. J.* **743**, 28 (2011).
 [3] P. J. E. Peebles, *Astrophys. J.* **284**, 439 (1984).
 [4] B. Ratra and M. S. Vogeley, *Publ. Astron. Soc. Pac.* **120**, 235 (2008).
 [5] E. Komatsu *et al.*, *Astrophys. J. Suppl. Ser.* **192**, 18 (2011).
 [6] D. J. Fixsen, *Astrophys. J.* **707**, 916 (2009).
 [7] G. Mangano, G. Miele, S. Pastor, T. Pinto, O. Pisanti, and P. D. Serpico, *Nucl. Phys.* **B729**, 221 (2005).
 [8] M. Archidiacono, E. Calabrese, and A. Melchiorri, *Phys. Rev. D* **84**, 123008 (2011).
 [9] Z. Hou, R. Keisler, L. Knox, M. Millea, and C. Reichardt, [arXiv:1104.2333](https://arxiv.org/abs/1104.2333).
 [10] T. L. Smith, S. Das, and O. Zahn, *Phys. Rev. D* **85**, 023001 (2012).
 [11] S. Hannestad, A. Mirizzi, G. G. Raffelt, I. Tambora, and Y. Y. Y. Wong, *Phys. Rev. Lett.* **105**, 181301 (2010); *J. Cosmol. Astropart. Phys.* **08** (2010) 001; L. M. Krauss, C. Lunardini, and C. Smith, [arXiv:1009.4666](https://arxiv.org/abs/1009.4666); K. Nakayama, F. Takahashi, and T. T. Yanagida, *Phys. Lett. B* **697**, 275 (2011); E. Calabrese, D. Huterer, E. V. Linder, A. Melchiorri, and L. Pagano, *Phys. Rev. D* **83**, 123504 (2011); E. Giusarma, M. Corsi, M. Archidiacono, R. de Putter, A. Melchiorri, O. Mena, and S. Pandolfi, *Phys. Rev. D* **83**, 115023 (2011); W. Fischler and J. Meyers, *Phys. Rev. D* **83**, 063520 (2011); P. C. de Holanda and A. Yu. Smirnov, *Phys. Rev. D* **83**, 113011 (2011); J. Hasenkamp, *Phys. Lett. B* **707**, 121 (2012); J. L. Menestrina and R. J. Scherrer, *Phys. Rev. D* **85**, 047301 (2012); T. Kobayashi, F. Takahashi, T. Takahashi, and M. Yamaguchi, *J. Cosmol. Astropart. Phys.* **03** (2012) 036; D. Hooper, F. S. Queiroz, and N. Y. Gnedin, *Phys. Rev. D* **85**, 063513 (2012); E. Giusarma, M. Archidiacono, R. de Putter, A. Melchiorri, and O. Mena, *Phys. Rev. D* **85**, 083522 (2012); M. Blennow, E. Fernandez-Martinez, O. Mena, J. Redondo, and P. Serra, *J. Cosmol. Astropart. Phys.* **07** (2012) 022; O. E. Bjælde, S. Das, and A. Moss, [arXiv:1205.0553](https://arxiv.org/abs/1205.0553).
 [12] S. Hannestad, A. Mirizzi, G. G. Raffelt, and Y. Y. Y. Wong, *J. Cosmol. Astropart. Phys.* **08** (2010) 001; A. Melchiorri, O. Mena, and A. Slosar, *Phys. Rev. D* **76**, 041303 (2007); T. L. Smith, E. Pierpaoli, and M. Kamionkowski, *Phys. Rev. Lett.* **97**, 021301 (2006); P. Binetruy, C. Deffayet, U. Ellwanger, and D. Langlois, *Phys. Lett. B* **477**, 285 (2000); T. Shiromizu, K. i. Maeda, and M. Sasaki, *Phys. Rev. D* **62**, 024012 (2000); S. Mukohyama, *Phys. Lett. B* **473**, 241 (2000), doi: [10.1016/S0370-2693\(99\)01505-1](https://doi.org/10.1016/S0370-2693(99)01505-1).
 [13] A. G. Riess, L. Macri, S. Casertano, H. Lampeitl, H. C. Ferguson, A. V. Filippenko, S. W. Jha, W. Li, and R. Chornock, *Astrophys. J.* **730**, 119 (2011).

- [14] G. A. Tammmman, A. Sandage, and B. Reindl, *Astron. Astrophys. Rev.* **15**, 289 (2008).
- [15] G. Chen and B. Ratra, *Astrophys. J.* **612**, L1 (2004); L. Samushia, G. Chen, and B. Ratra, [arXiv:0706.1963](#); L. Samushia and B. Ratra, *Astrophys. J.* **680**, L1 (2008).
- [16] J. R. Gott, III, M. S. Vogeley, S. Podariu, and B. Ratra, *Astrophys. J.* **549**, 1 (2001).
- [17] M. Kowalski *et al.*, *Astrophys. J.* **686**, 749 (2008); A. Barreira and P. P. Avelino, *Phys. Rev. D* **84**, 083521 (2011).
- [18] S. Podariu, T. Souradeep, J. R. Gott, III, B. Ratra, and M. S. Vogeley, *Astrophys. J.* **559**, 9 (2001).
- [19] G. Chen and B. Ratra, *Publ. Astron. Soc. Pac.* **115**, 1143 (2003).
- [20] G. Chen, J. R. Gott, III, and B. Ratra, *Publ. Astron. Soc. Pac.* **115**, 1269 (2003).
- [21] G. Chen and B. Ratra, *Publ. Astron. Soc. Pac.* **123**, 1127 (2011).
- [22] A. Lewis and S. Bridle, *Phys. Rev. D* **66**, 103511 (2002).
- [23] C. L. Reichardt *et al.*, *Astrophys. J.* **694**, 1200 (2009).
- [24] B. A. Reid, W. J. Percival, D. J. Eisenstein, L. Verde, D. N. Spergel, R. A. Skibba, N. A. Bahcall, and T. Budavari *et al.*, *Mon. Not. R. Astron. Soc.* **404**, 60 (2010).
- [25] B. Ratra, *Phys. Rev. D* **43**, 3802 (1991); S. Podariu and B. Ratra, *Astrophys. J.* **532**, 109 (2000).
- [26] P. J. E. Peebles and B. Ratra, *Astrophys. J.* **325**, L17 (1988); B. Ratra and P. J. E. Peebles, *Phys. Rev. D* **37**, 3406 (1988).
- [27] A. Vikhlinin *et al.*, *Astrophys. J.* **692**, 1060 (2009).
- [28] S. Joudaki, [arXiv:1202.0005](#).
- [29] G. Mangano and P. D. Serpico, *Phys. Lett. B* **701**, 296 (2011).
- [30] R. Kessler *et al.*, *Astrophys. J. Supp.* **185**, 32 (2009).